Indonesian Journal of Material Research
***e*-ISSN: 2987-1654**
Vol. 4, No. 2, July 2026

Indonesian Journal of MATERIAL RESEARCH

Research Paper

Hydrothermal Fabrication of NiAl-LDH Coupled with Spirulina Hydrochar for Efficient Photodegradation of Methylene Blue

Navinda Ramadhan[1,2*], Komis Komis[1,2], Novita Sari[1,2], Normah Normah [2,3]

[1] *Master Program of Materials Science, Graduate School, Universitas Sriwijaya, Palembang, South Sumatra 30139, Indonesia*
[2] *Research Center of Inorganic Materials and Coordination Complexes, Universitas Sriwijaya, Palembang South Sumatra 30139, Indonesia*
[3] *Departement of Chemistry, Universitas Indo Global Mandiri, Palembang, South Sumatra, 30129, Indonesia*
[*]**Corresponding author**: navindaramadhanofficial@gmail.com

Abstract
In this study, a Ni/Al layered double hydroxide (LDH) coupled with Spirulina-derived hydrochar was successfully synthesized via a microwave-assisted hydrothermal method for the photodegradation of methylene blue (MB) under visible light irradiation. The incorporation of hydrochar significantly modified the structural, surface, and optical properties of Ni/Al-LDH, resulting in enhanced photocatalytic performance. Characterization results confirmed the successful formation of the composite with improved surface area and extended light absorption. Photodegradation experiments revealed that the Ni/Al-Spirulina composite exhibited superior performance compared to pristine Ni/Al-LDH, achieving higher degradation efficiency under various conditions. The enhanced activity was influenced by operational parameters such as pH, catalyst dosage, and initial dye concentration, with optimal performance observed under near-neutral conditions. The improved performance is attributed to the synergistic effect between adsorption and photocatalysis, where hydrochar facilitates charge separation and promotes the generation of reactive oxygen species. Overall, this study demonstrates an effective strategy for developing biomass-based LDH composites as efficient and sustainable photocatalysts for wastewater treatment.

Keywords
NiAl-LDH, Spirulina Hydrochar, Photodegradation, Visible Light, Dye Removal

Received: 29 January 2026, Accepted: 8 April 2026
https://doi.org/10.26554/ijmr.20264290

1. INTRODUCTION

Layered double hydroxides (LDH) are a class of two-dimensional anionic clays characterized by a brucite-like layered structure and exchangeable interlayer anions (Rath et al., 2025). The general formula of LDHs can be expressed as $[M^{2+}_{(1-x)}M^{3+}_{(x)}(OH)_2]^{x+}(A^{n-})_{x/n}.mH_2O$ where M^{2+} and M^{3+} represent divalent and trivalent metal cations, respectively, and A^{n-} denotes the interlayer anion (Memon et al., 2021; Upadhyay and Chakma, 2024). This unique structure enables LDHs to exhibit high surface reactivity, tunable composition, and excellent adsorption-catalysis properties (Eltaweil et al., 2025). Among various LDH systems, NiAl-LDH has gained considerable attention due to its favorable redox properties associated with Ni species and its relatively high structural stability, making it a potential candidate for photocatalytic applications (Palapa et al., 2024).

Despite these advantages, pristine NiAl-LDH still suffers from several intrinsic limitations, including limited specific surface area and the rapid recombination of photogenerated electron-hole pairs (Al-musawi et al., 2024), which significantly reduce its photocatalytic efficiency (Nour and Nabwey, 2025). Furthermore, the stacking of LDH layers often restricts the accessibility of active sites, thereby limiting its interaction with target pollutants (Fu et al., 2025). Therefore, rational material design is required to overcome these drawbacks and enhance its overall performance.

One promising strategy is the integration of LDH with carbonaceous materials, particularly hydrochar derived from biomass (Amri et al., 2023; Ramadhan et al., 2025). Hydrochar typically possesses abundant oxygen-containing functional groups (–OH, –COOH) (Oyebamiji et al., 2025), porous structures (Zahid et al., 2025), and good electron conductivity (Zauška et al., 2024), which can facilitate pollutant adsorption and improve charge separation. In this context, Spirulina platensis, a nitrogen-rich microalgae (Ramadhan et al., 2025), represents a highly attractive precursor due to its intrinsic heteroatom content that can introduce additional active sites and improve the electronic properties of the resulting hydrochar (Chwil et al., 2024; Zhang et al., 2021). The incorporation of such hydrochar into NiAl-LDH is expected to not only increase the surface area but also create interfacial interactions that promote electron transfer and suppress recombination processes (Ramadhan et al., 2026).

In addition to material composition, the synthesis approach

plays a crucial role in determining the physicochemical properties of the composite (Badaruddin et al., 2022). Microwave-assisted hydrothermal synthesis has emerged as an advanced method offering rapid and uniform heating (Han et al., 2024), reduced synthesis time, and enhanced nucleation efficiency compared to conventional hydrothermal techniques (Ashiq et al., 2021). This method facilitates better dispersion of LDH layers onto the hydrochar matrix and promotes stronger interfacial contact, which is essential for achieving synergistic photocatalytic performance (Meng et al., 2025).

Although several studies have reported LDH-based composites for pollutant removal, the integration of NiAl-LDH with Spirulina-derived hydrochar via a microwave-assisted hydrothermal route remains relatively unexplored. The novelty of this study lies in the combined utilization of (i) nitrogen-rich microalgae derived hydrochar as a functional support, (ii) Ni-based LDH with tunable layered structure, and (iii) a microwave-assisted synthesis strategy to enhance interfacial interaction and catalytic efficiency. This integrated approach is expected to provide a synergistic effect that significantly improves photocatalytic activity. Methylene blue (MB), a widely used cationic dye in textile and industrial processes, is often detected in wastewater and poses serious environmental risks due to its stability and toxicity. Photodegradation is considered an effective and environmentally benign technique for the removal of such organic contaminants. Therefore, the development of efficient photocatalysts based on advanced composite materials is of great importance.

In this study, a Ni/Al-Spirulina derived hydrochar composite was synthesized via a microwave-assisted hydrothermal method. The structural, morphological, and surface properties of the prepared materials were characterized using XRD, FTIR, UV-DRS, SEM, and BET analyses. Furthermore, the photocatalytic performance of the composite was evaluated through the degradation of methylene blue, followed by kinetic analysis and investigation of the underlying degradation mechanism.

2. EXPERIMENTAL SECTION

2.1 Materials and Equipment

Nickel(II) nitrate hexahydrate ($Ni(NO_3)_2.6H_2O$, FW = 290.79 $g.mol^{-1}$, Merck, Germany), aluminum nitrate nonahydrate ($Al(NO_3)_3.9H_2O$, FW = 375.13 $g.mol^{-1}$, Merck, Germany), sodium hydroxide (NaOH, FW = 40.00 $g.mol^{-1}$, Merck, Germany), hydrochloric acid (HCl, 37%, FW = 36.46 $g.mol^{-1}$, Merck, Germany), and sodium chloride (NaCl, FW = 58.44 $g.mol^{-1}$, Merck, Germany) were used as received without further purification. Methylene blue ($C_{16}H_{18}ClN_3S$, analytical grade) was used as the target pollutant in the photodegradation experiments. *Spirulina platensis* powder (analytical grade), obtained from Maluku, Indonesia, was used as the precursor for hydrochar preparation.

The main instruments used in this study included an analytical balance (US Solid), a drying oven (B-One, Germany), and a microwave oven (Sharp, Japan) for microwave-assisted synthesis. A Teflon-lined stainless-steel autoclave was used for the hydrothermal process. The structural properties of the materials were analyzed using X-ray diffraction (XRD, Rigaku Miniflex-6000, 5–90°). Functional groups were identified using Fourier transform infrared spectroscopy (FTIR, Shimadzu Prestige-21, 400–3800 cm^{-1}). Surface area and porosity were determined using a Brunauer–Emmett–Teller (BET) analyzer (BELSORP-miniX). Morphological analysis was conducted using scanning electron microscopy (SEM, JEOL JSM-6510LA). The concentration of methylene blue during photodegradation was measured using a UV-visible spectrophotometer (EMC Lab-18 PC).

2.2 Synthesis of Materials

Hydrochar from Spirulina was synthesized using a microwave-assisted hydrothermal carbonization (Elshishini et al., 2024). In a typical procedure, 2.5 g of Spirulina powder was dispersed in 50 mL of deionized water and stirred to obtain a homogeneous suspension. The mixture was then transferred into a Teflon-lined sealed vessel suitable for microwave processing. The suspension was treated under microwave irradiation at a power of 1000 W for 90 minutes. After completion of the reaction, the system was allowed to cool naturally to room temperature. The resulting solid product was separated by filtration, washed several times with deionized water until neutral pH was reached, and dried in an oven at 60 °C for 6 hours. The dried hydrochar was then ground into a fine powder and used for further synthesis.

The Ni/Al-Spirulina composite was prepared via a microwave-assisted co-precipitation followed by in-situ crystallization. Nickel(II) nitrate hexahydrate and aluminum nitrate nonahydrate were dissolved in deionized water at a molar ratio of 3:1 to form a mixed metal precursor solution. The pH of the solution was adjusted to 10 by the dropwise addition of 2 M NaOH under continuous stirring. Subsequently, 1 g of the prepared hydrochar was added into the solution, and the mixture was stirred until a uniform suspension was achieved. The suspension was then transferred into a Teflon-lined stainless-steel autoclave and subjected to microwave irradiation at 300 W for 30 minutes to facilitate rapid crystallization of NiAl-LDH onto the hydrochar surface.

After the reaction, the mixture was allowed to cool naturally to room temperature. The obtained solid was collected by filtration, thoroughly washed with deionized water until neutral pH, and dried at 60 °C for 6 hours. Finally, the dried composite was ground into a fine powder and stored for subsequent characterization and photodegradation experiments.

2.3 Characterization

The crystalline structure of the synthesized materials was analyzed using X-ray diffraction (XRD, Rigaku Miniflex-6000) in the 2θ range of 5–90°. Functional groups and chemical bonding were identified using Fourier transform infrared spectroscopy (FTIR, Shimadzu Prestige-21) within the wavenumber range of 400–3800 cm^{-1}. The surface morphology and particle distribution were observed using scanning electron microscopy (SEM, JEOL JSM-6510LA). The specific surface area and pore structure of the samples were determined using the Brunauer–Emmett–Teller (BET) method with a BELSORP-miniX surface area analyzer.

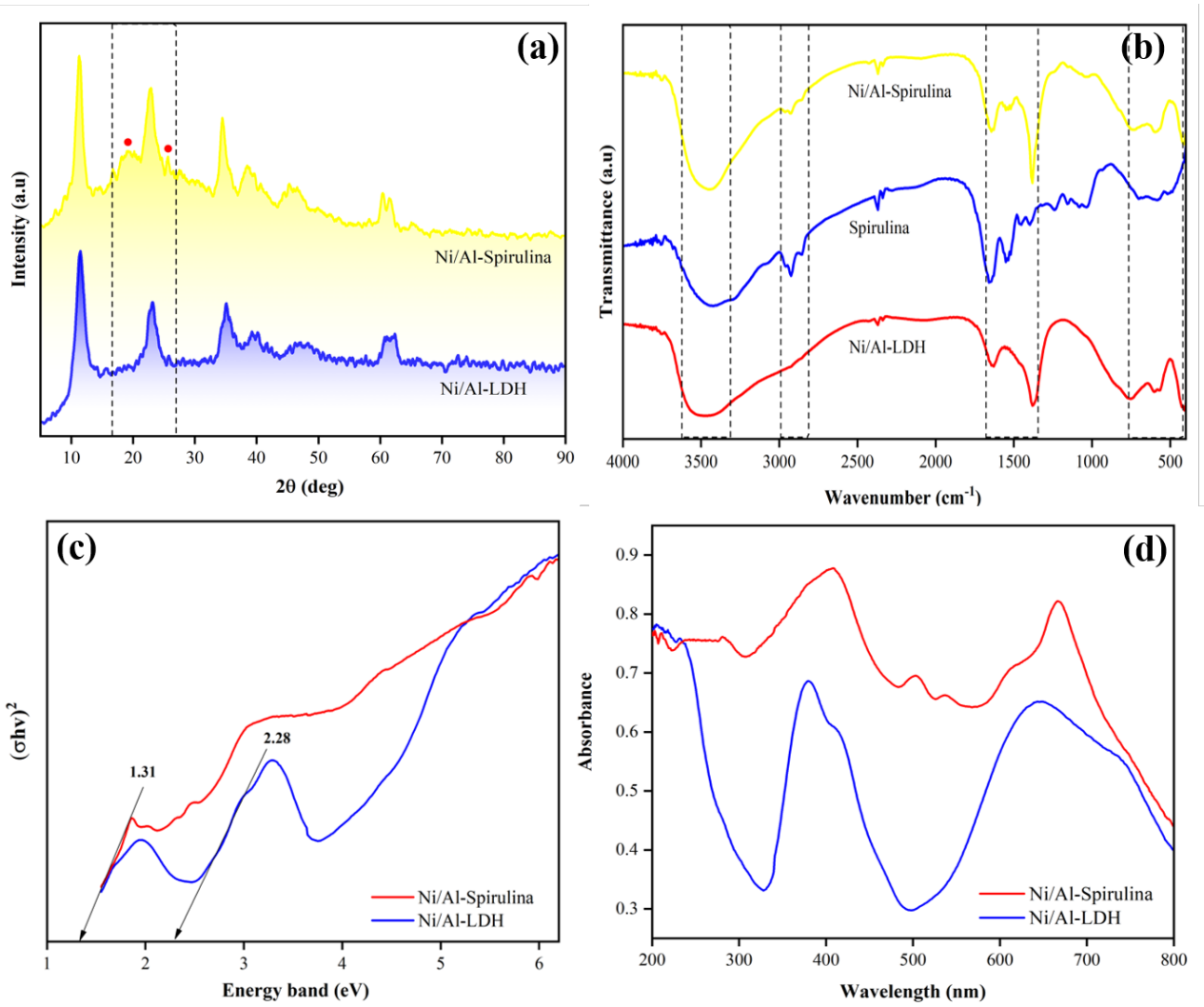

Figure 1. (a) XRD Patterns, (b) FTIR Spectra, (c) Tauc Plots Derived from UV-Vis DRS, and (d) UV-Vis Absorption Spectra of Ni/Al-LDH and Ni/Al-Spirulina

Prior to analysis, all samples were degassed to remove moisture and impurities. The optical properties of the materials were evaluated using UV-Vis diffuse reflectance spectroscopy (UV-Vis DRS, Jasco V-760). The absorption data were used to estimate the band gap energy of the samples.

2.4 Photodegradation Experiment

The photocatalytic activity of the synthesized materials was evaluated through the degradation of methylene blue (MB) under visible light irradiation (Amri et al., 2026). In a typical experiment, 0.02 g of catalyst was dispersed in 20 mL of MB solution with a predetermined initial concentration. The suspension was magnetically stirred in the dark for 30 minutes to establish adsorption-desorption equilibrium.

After reaching equilibrium, the suspension was irradiated using a visible light source (14 W) positioned at a distance of 25 cm from the solution surface, while continuous stirring was maintained. At predetermined time intervals, aliquots were withdrawn and centrifuged to separate the catalyst particles. The concentration of MB in the supernatant was determined using a UV-Vis spectrophotometer at its maximum absorption wavelength. The degradation efficiency (%) was calculated using the following Equation 1.

$$\%Degradation = \frac{(C_0 - C_t)}{C_0} \times 100 \quad (1)$$

where C_0 represents the initial concentration of MB and C_t is the concentration at irradiation time t. The photocatalytic kinetics were analyzed using a pseudo-first-order model, expressed as Equation 2.

$$\ln\left(\frac{C_0}{C_t}\right) = kt \quad (2)$$

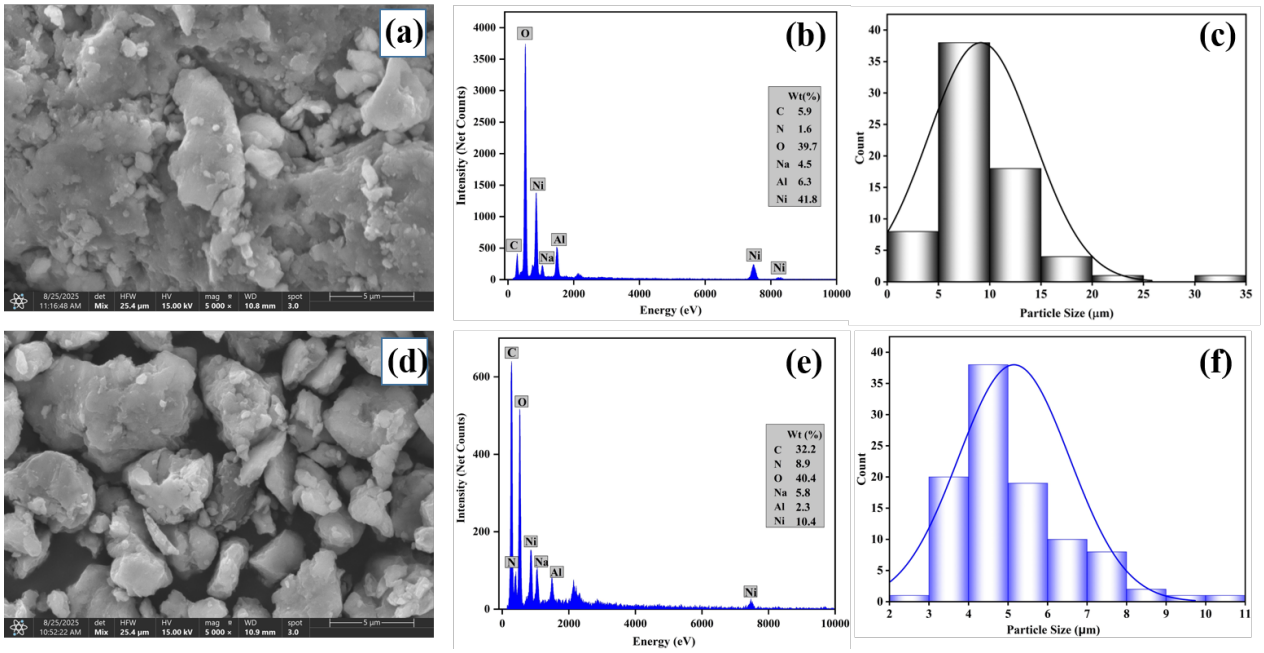

Figure 2. (a-c) SEM Image, EDS Spectrum, and Particle Size Distribution of Ni/Al-LDH; (d–f) SEM Image, EDS Spectrum, and Particle Size Distribution of Ni/Al-Spirulina

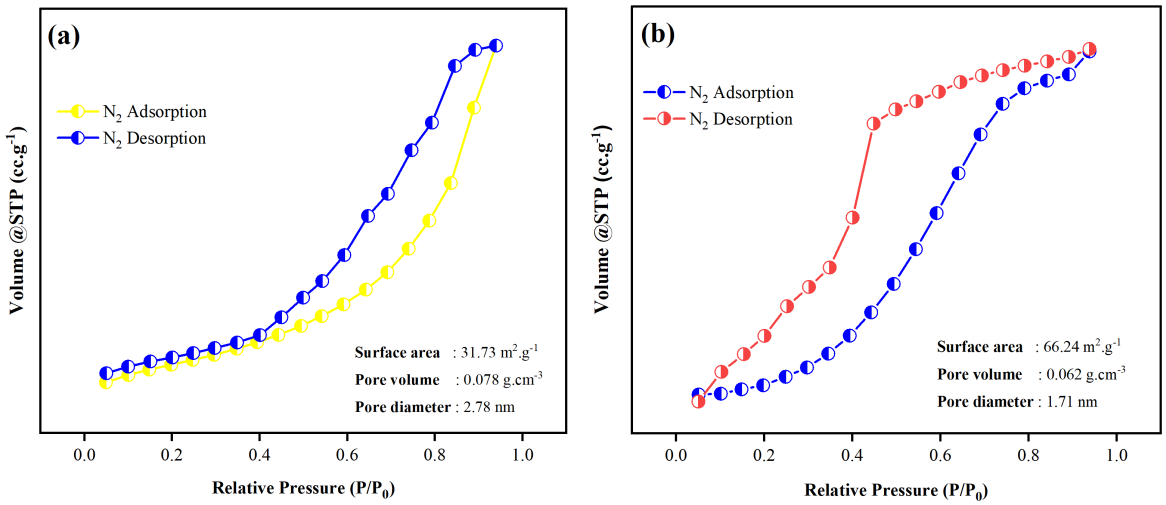

Figure 3. N_2 Adsorption-Desorption Isotherms of (a) NiAl-LDH and (b) NiAl-Spirulina Hydrochar Composite

where k is the apparent rate constant (min^{-1}) and t is the irradiation time (min). All experiments were carried out under identical conditions to ensure consistency and reproducibility of the results.

3. RESULTS AND DISCUSSION

3.1 Characterization of Materials

The crystalline structure of the synthesized materials was investigated using X-ray diffraction (Figure 1a). The NiAl-LDH sample exhibits characteristic reflections at low diffraction angles, which can be indexed to the (003), (006), and (009) planes (Ramadhan et al., 2025), confirming the formation of a typical layered double hydroxide structure (Palapa et al., 2024). These reflections indicate a well-ordered lamellar arrangement. After incorporation of Spirulina-derived hydrochar, the overall diffraction pattern remains preserved, indicating that the LDH structure is maintained. However, a reduction in peak intensity and slight peak broadening are observed in the composite, suggesting decreased

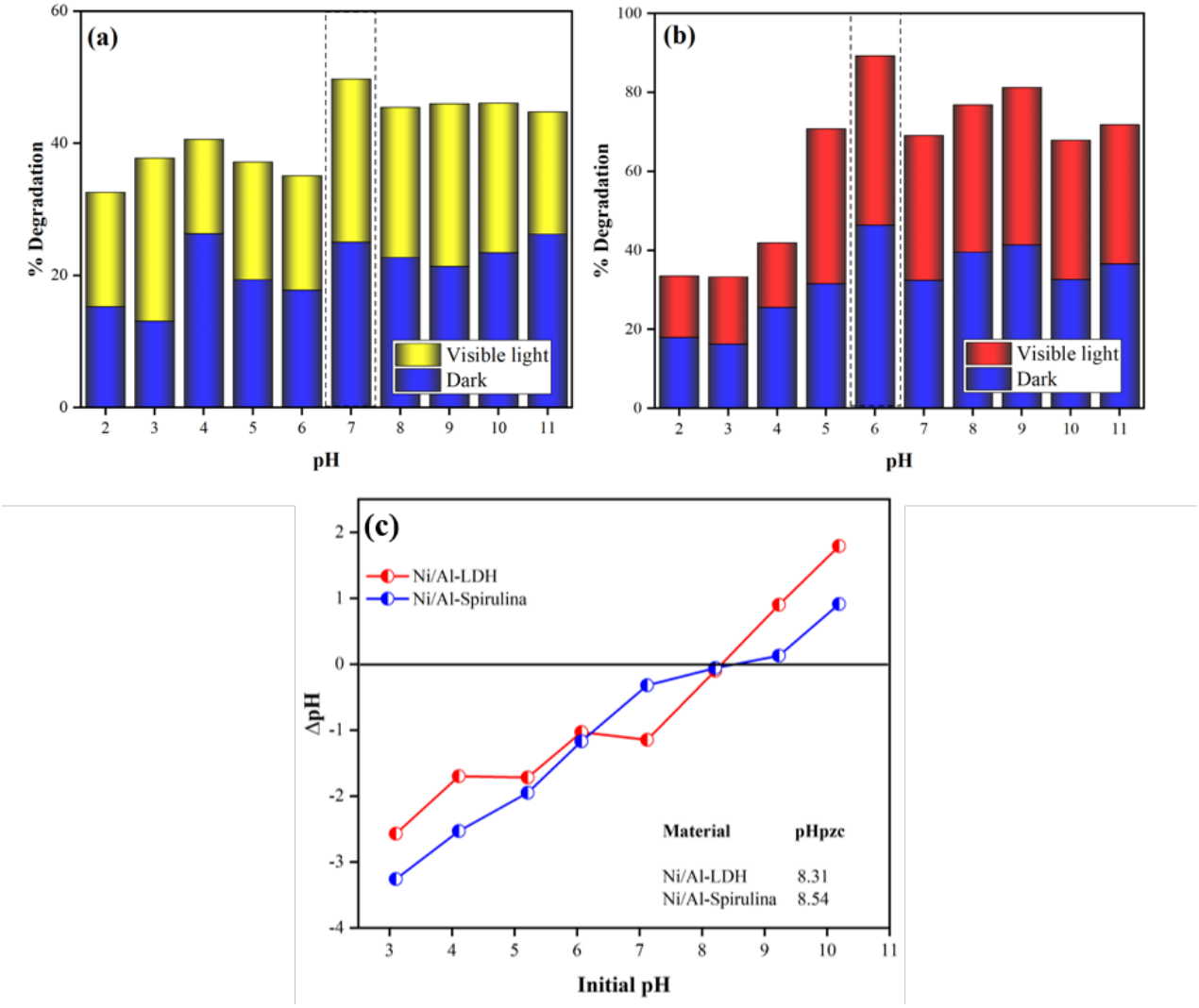

Figure 4. Effect of Initial pH on MB Degradation: (a) Ni/Al-LDH, (b) Ni/Al-Spirulina Under Dark and Visible Light Conditions, and (c) Determination of pHpzc for Both Materials

crystallinity and partial disruption of layer stacking. This behavior is attributed to the interaction between LDH nanosheets and the amorphous carbon matrix, which inhibits crystal growth and enhances dispersion. The increased amorphous background further confirms the successful integration of hydrochar into the LDH structure.

The chemical properties of the materials were analyzed using FTIR spectroscopy (Figure 1b). The NiAl-LDH spectrum shows a broad band around 3400 cm^{-1}, corresponding to the stretching vibration of hydroxyl groups from the layered structure and interlayer water molecules. The band observed in the range of 1350-1500 cm^{-1} is associated with interlayer carbonate anions, while the region below 800 cm^{-1} corresponds to metal–oxygen vibrations (Ni–O and Al–O). The hydrochar exhibits characteristic bands related to oxygen-containing functional groups such as hydroxyl, carbonyl, and C–O groups. In the composite material, the presence of both LDH and hydrochar features is clearly observed, accompanied by slight shifts in peak positions and changes in intensity. These variations indicate the presence of interfacial interactions between the two components, which are beneficial for charge transfer during photocatalytic reactions.

Optical absorption properties were evaluated using UV-Vis diffuse reflectance spectroscopy as demonstrated in Figure 1d. The NiAl-LDH sample shows relatively limited absorption in the visible region, whereas the Ni/Al-Spirulina composite demonstrates enhanced absorption over a wider wavelength range. This improvement is attributed to the incorporation of hydrochar, which increases light-harvesting capability and promotes better utilization of visible light. The band gap energies were estimated from Tauc plots (Figure 1c). The pristine NiAl-LDH exhibits a relatively wide band gap, which limits its activity under visible light irradiation. In contrast, the composite shows a reduced

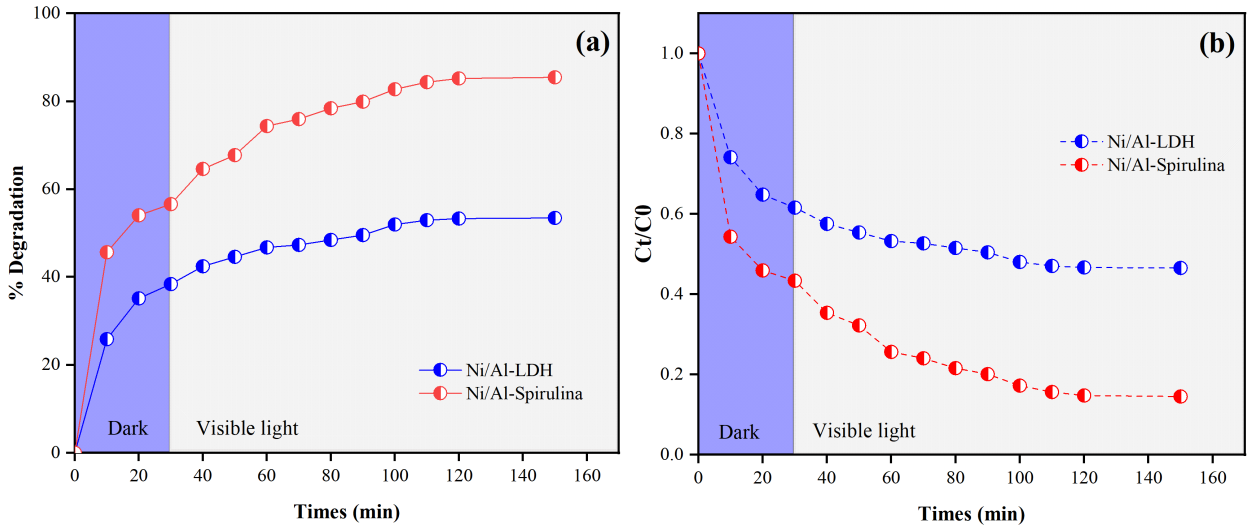

Figure 5. (a) Degradation Efficiency and (b) Ct/C0 Profile of MB Over Time Under Dark and Visible Light Irradiation

band gap of approximately 2.28 eV, along with an additional lower-energy transition around 1.31 eV. This reduction indicates that the electronic structure has been modified by the presence of hydrochar, leading to the formation of additional energy states. These states facilitate electron excitation under lower photon energy and help suppress electron-hole recombination. Overall, the combination of structural modification, surface functional groups, and band gap reduction demonstrates a synergistic interaction between NiAl-LDH and Spirulina-derived hydrochar. This synergy is expected to significantly enhance photocatalytic performance under visible light irradiation.

The surface morphology of NiAl-LDH and NiAl-Spirulina composite was examined using SEM, as presented in Figures 2a and 2d. The pristine NiAl-LDH exhibits a typical aggregated platelet-like structure, where the particles tend to stack and form dense agglomerates. This morphology is characteristic of LDH materials due to strong interlayer interactions and hydrogen bonding, which often limit the accessibility of active sites (Arieveali et al., 2026). In contrast, the Ni/Al-Spirulina composite shows a more fragmented and loosely packed morphology with reduced agglomeration. The particles appear more dispersed and irregular, indicating that the presence of hydrochar effectively inhibits the restacking of LDH layers. This structural modification is crucial, as it can enhance the exposure of active sites and facilitate mass transfer during photocatalytic reactions.

The elemental composition was further analyzed using EDS (Figures 2b and 2e). The NiAl-LDH sample primarily consists of Ni, Al, and O elements, confirming the successful formation of the LDH structure. Meanwhile, the composite material shows a significant increase in carbon content, along with the presence of nitrogen, which originates from the Spirulina-derived hydrochar. This result confirms the successful incorporation of hydrochar into the LDH matrix. The presence of nitrogen-containing functional groups is particularly beneficial, as it can introduce additional active sites and improve electron mobility.

The particle size distribution analysis (Figures 2c and 2f) reveals a clear difference between the two materials. NiAl-LDH exhibits a broader size distribution with relatively larger particle sizes, indicating significant aggregation. In contrast, the composite displays a narrower distribution with smaller average particle size. This reduction in particle size is attributed to the role of hydrochar as a structural modifier, which limits particle growth during synthesis and promotes better dispersion.

The textural properties of the synthesized materials were evaluated using N_2 adsorption-desorption isotherms, as presented in Figure 3. Both samples exhibit type IV isotherms with noticeable hysteresis loops, indicating the presence of mesoporous structures. This mesoporosity is essential for facilitating mass transfer and improving the accessibility of active sites during photocatalytic reactions (Zheng et al., 2022). The pristine NiAl-LDH (Figure 3a) shows a relatively moderate adsorption capacity with a specific surface area of 31.73 $m^2.g^{-1}$, pore volume of 0.078 $cm^3.g^{-1}$, and an average pore diameter of 2.78 nm. The isotherm profile suggests limited pore development, which is consistent with the aggregated layered structure observed in the SEM analysis.

In contrast, the Ni/Al-Spirulina composite (Figure 3b) exhibits a significantly enhanced adsorption capacity, reflected by an increase in surface area to 66.24 $m^2.g^{-1}$. Although the pore volume slightly decreases to 0.062 $cm^3\ g^{-1}$, the average pore diameter is reduced to 1.71 nm, indicating the formation of smaller and more uniformly distributed pores. The presence of a more pronounced hysteresis loop further suggests improved pore connectivity and structural heterogeneity (Liu et al., 2024). The substantial increase in surface area is attributed to the incorporation of hydrochar, which acts as a porous scaffold and prevents the restacking of LDH layers. This results in better dispersion and the generation of additional accessible surface sites. The

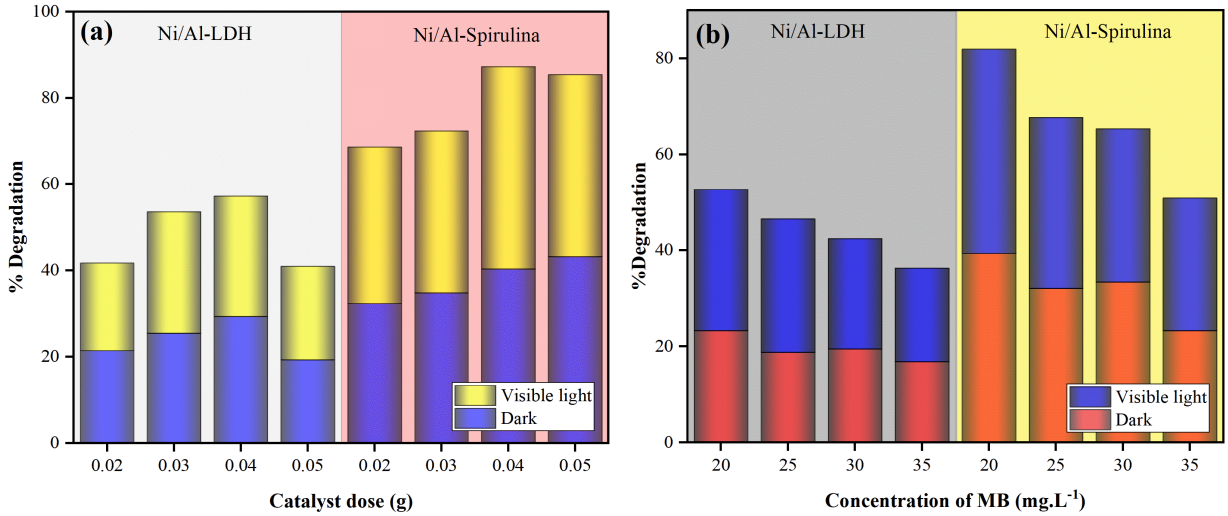

Figure 6. Effect of (a) Catalyst Dosage and (b) Initial MB Concentration on Degradation Efficiency Under Dark and Visible Light Conditions

reduction in pore diameter, combined with increased surface area, suggests the formation of a hierarchical porous structure that is beneficial for adsorption-photocatalysis synergy.

Overall, the modification of NiAl-LDH with Spirulina-derived hydrochar leads to significant improvement in textural properties, particularly surface area and pore structure. These enhancements are expected to play a crucial role in improving photocatalytic efficiency by increasing pollutant adsorption capacity and facilitating faster diffusion of reactant molecules to active sites.

3.2 Effect of pH

The influence of initial pH on methylene blue (MB) degradation is presented in Figure 4a-b. Under dark conditions, both materials show moderate removal due to adsorption, which increases toward near-neutral pH. Upon visible light irradiation, degradation efficiency significantly improves, confirming the dominant role of photocatalysis. Ni/Al-Spirulina exhibits consistently higher performance than pristine Ni/Al-LDH across all pH values, with optimum activity observed around pH 6–7. This enhancement is attributed to the synergistic effect between adsorption and photocatalysis, where hydrochar improves pollutant affinity and promotes charge separation.

At acidic pH, reduced efficiency is associated with surface protonation and electrostatic repulsion with cationic MB. Meanwhile, at alkaline conditions, the performance tends to stabilize due to possible radical scavenging by excess hydroxide ions. The pHpzc results (Figure 4c) indicate values of 8.31 (Ni/Al-LDH) and 8.54 (Ni/Al-Spirulina), suggesting that surface charge plays a role in adsorption behavior. However, the highest degradation at near-neutral pH implies that photocatalytic activity is governed not only by electrostatic interaction but also by efficient charge transfer within the composite system.

3.3 Effect of Contact Time

The degradation behavior of methylene blue (MB) as a function of contact time is illustrated in Figure 5a–b. During the dark phase (0–30 min), both materials exhibit a noticeable decrease in MB concentration, indicating that adsorption plays an important role prior to irradiation. The Ni/Al-Spirulina composite shows higher initial removal compared to Ni/Al-LDH, suggesting that the incorporation of hydrochar enhances adsorption capacity due to the presence of porous structure and oxygen/nitrogen-containing functional groups (Rohmatullaili et al., 2024).

Upon visible light irradiation, a significant enhancement in degradation efficiency is observed for both samples. The Ni/Al-Spirulina composite consistently outperforms pristine Ni/Al-LDH, reaching approximately 85% degradation after 150 minutes, whereas Ni/Al-LDH achieves only about 53%. This substantial difference confirms the synergistic effect between adsorption and photocatalysis, where hydrochar not only improves pollutant accumulation near active sites but also facilitates charge transfer, thereby suppressing electron-hole recombination.

The degradation profile shows a rapid decrease in MB concentration during the initial irradiation stage, followed by a slower rate at longer reaction times. This behavior indicates that the process is initially governed by abundant active sites and reactive species generation, while at later stages it becomes limited by reduced pollutant concentration and possible occupation of active sites. This trend is further supported by the *Ct/C0* profile (Figure 5b), where the composite exhibits a more pronounced decline, reflecting faster reaction kinetics. Overall, the enhanced performance of Ni/Al-Spirulina can be attributed to the combined effects of improved adsorption capability (Ajduković et al., 2023), increased surface area, and enhanced interfacial charge transfer. These factors collectively contribute to a more efficient

photocatalytic system compared to pristine Ni/Al-LDH.

3.4 Effect of Catalyst Dose and Initial Concentration

The influence of catalyst dosage and initial methylene blue (MB) concentration on degradation efficiency is presented in Figure 6a–b. As shown in Figure 6a, the degradation efficiency increases with increasing catalyst dose for both materials. This trend is attributed to the higher availability of active sites and enhanced light absorption, which promote the generation of reactive species (Kundu and Naskar, 2021). The Ni/Al-Spirulina composite exhibits consistently higher performance than Ni/Al-LDH at all dosages, reaching optimal efficiency at 0.04 g. A slight decrease at 0.05 g suggests that excessive catalyst loading may induce light scattering and reduce effective photon penetration, thereby limiting photocatalytic activity.

Figure 6b shows the effect of initial MB concentration. The degradation efficiency decreases with increasing dye concentration for both samples. At higher concentrations, the number of MB molecules exceeds the available active sites, and the solution becomes more optically dense, which hinders light penetration and reduces the generation of reactive species. Despite this limitation, Ni/Al-Spirulina maintains superior performance across all concentrations, indicating its enhanced adsorption-photocatalysis synergy.

The improved performance of the composite can be attributed to the presence of hydrochar, which increases surface area, provides additional adsorption sites, and facilitates charge transfer. These factors enable the composite to better accommodate higher pollutant loading while maintaining efficient photocatalytic activity.

3.5 Photodegradation Mechanism

Based on the structural, optical, and photocatalytic results, a plausible mechanism for MB degradation over the Ni/Al-Spirulina composite is proposed. Under visible light irradiation, the Ni/Al-LDH component absorbs photons and generates electron–hole pairs (e^-/h^+). However, in pristine LDH, rapid recombination limits its photocatalytic efficiency (Amri et al., 2026). In the composite system, the presence of Spirulina-derived hydrochar plays a crucial role as an electron mediator. The photogenerated electrons from Ni/Al-LDH can be effectively transferred to the conductive hydrochar matrix, which suppresses charge recombination and prolongs the lifetime of charge carriers. This enhanced charge separation significantly improves photocatalytic activity.

The transferred electrons react with dissolved oxygen to generate superoxide radicals ($\cdot O_2^-$), while photogenerated holes (h^+) can directly oxidize MB or react with water molecules to produce hydroxyl radicals ($\cdot OH$) (Arieveali et al., 2026). These reactive oxygen species are responsible for the oxidative degradation of MB into smaller, less harmful intermediates and eventually mineralized products. Additionally, the nitrogen-containing functional groups from Spirulina-derived hydrochar contribute to improved electron density and facilitate interfacial charge transfer. Combined with increased surface area and adsorption capability, the composite ensures higher pollutant concentration near active sites, further enhancing degradation efficiency. Overall, the superior performance of Ni/Al-Spirulina can be attributed to the synergistic effects of (i) improved light absorption, (ii) efficient charge separation via hydrochar, and (iii) enhanced adsorption–photocatalysis coupling, resulting in a more effective degradation pathway compared to pristine Ni/Al-LDH.

4. CONCLUSIONS

In this study, a Ni/Al-LDH coupled with Spirulina-derived hydrochar was successfully synthesized via a microwave-assisted hydrothermal method and demonstrated enhanced performance for the photodegradation of methylene blue under visible light. The incorporation of hydrochar improved surface area, adsorption capacity, and light absorption, while facilitating charge transfer and suppressing electron–hole recombination. As a result, the composite exhibited significantly higher degradation efficiency compared to pristine Ni/Al-LDH under various experimental conditions. The performance was influenced by operational parameters such as pH, catalyst dosage, and initial dye concentration, with optimal degradation observed under near-neutral conditions and moderate catalyst loading. Mechanistically, the enhanced activity is attributed to the synergistic interaction between adsorption and photocatalysis, where hydrochar acts as an electron mediator to promote the formation of reactive oxygen species. These findings highlight the potential of biomass-derived hydrochar-LDH composites as efficient and sustainable photocatalysts for wastewater treatment applications.

5. ACKNOWLEDGEMENT

The authors gratefully acknowledge the Research Center of Inorganic Materials and Coordination Complexes, Universitas Sriwijaya, for providing research facilities and technical support.

REFERENCES

Ajduković, M., G. Stevanović, S. Marinović, Z. Mojović, P. Banković, K. Radulović, and N. Jović-Jovičić (2023). Ciprofloxacin Adsorption onto a Smectite–Chitosan-Derived Nanocomposite Obtained by Hydrothermal Synthesis. *Water*, **15**(14); 2608

Al-musawi, T. J., R. Rahimpoor, N. Mengelizadeh, and D. Balarak (2024). Enhanced Photocatalytic Degradation of Ciprofloxacin Antibiotics Using Fe_3O_4-SiO_2-EN @ Zn-Al Layered Double Hydroxide Nanocomposites Under the COVID-19 Pandemic. *Results in Engineering*, **24**; 103396

Amri, A., N. Annuria, M. Said, Y. Hanifah, and A. Lesbani (2026). Bio-functionalization of Zn/Al Layered Double Hydroxide Using Camellia sinensis Extract for Photocatalytic Ceftriaxone Degradation. *Sustainable Chemistry One World*, **10**; 100215

Amri, A., R. Rezonsi, N. Ahmad, T. Taher, and N. R. Palapa (2023). Biochar-Modified Layered Double Hydroxide for Highly Efficient on Phenol Adsorption. *Bulletin of Chemical Reaction Engineering & Catalysis*, **18**(3); 460–472

Arieveali, H., T. Taher, N. A. Fithri, N. Ahmad, and A. Lesbani (2026). Bookshelf-Inspired Norfloxacin Photooxidation Under UV/H_2O_2 Influence Using Microwave-Assisted Hydrothermal-Designed ZnAl/ZnO. *Surfaces and Interfaces*, **89**; 109181

Ashiq, A., M. Vithanage, B. Sarkar, M. Kumar, A. Bhatnagar, E. Khan, Y. Xi, and Y. Sik (2021). Carbon-Based Adsorbents for Fluoroquinolone Removal from Water and Wastewater: A Critical Review. *Environmental Research*, **197**; 111091

Badaruddin, M., N. Ahmad, E. S. Fitri, A. Lesbani, and R. Mohadi (2022). Hydrochar and Humic Acid as Template of ZnAl Layered Double Hydroxide for Adsorption of Phenol. *Science and Technology Indonesia*, **7**(4); 492–499

Chwil, M., R. Mihelič, R. Matraszek-Gawron, P. Terlecka, M. M. Skoczylas, and K. Terlecki (2024). Comprehensive Review of the Latest Investigations of the Health-Enhancing Effects of Selected Properties of Arthrospira and Spirulina Microalgae on Skin. *Pharmaceuticals*, **17**(10); 1321

Elshishini, H. M., G. M. Elsubruiti, Z. F. Ghatass, and A. S. Eltaweil (2024). Microwave-Assisted Synthesis of Zn–Fe LDH Modified with Magnetic Oxidized Hydrochar for Pb(II) Removal: Insights into Stability, Performance and Mechanism. *Journal of Solid State Chemistry*, **335**; 124689

Eltaweil, A. S., A. E. Awad, E. M. A. El-monaem, A. M. Shaker, and G. M. El-subruiti (2025). Rational Engineering of 3D Petal-Like Porous Magnetic $SnFe_2O_4$ / Boron Nitride / NiAl-LDH Composite for Pb(II) Ions Removal. *Journal of Molecular Structure*, **1337**; 142143

Fu, M., J. Xu, T. Lu, Q. Ma, Y. Luo, W. Feng, and X. Wang (2025). Synthesis and Characterization of N-Doped Seaweed Biochar and Removal of Cationic Dyes. *ACS Omega*

Han, X. W., S. Guo, X. Gao, C. Lu, and S. Wang (2024). Three-Dimensional Mg–Al Layered Double Hydroxide Decorated Reduced Graphene Oxide Nanocomposite: An Efficient Adsorbent for the Removal of Methylene Blue and Ciprofloxacin. *Applied Clay Science*, **250**; 107280

Kundu, S. and M. K. Naskar (2021). Carbon-Layered Double Hydroxide Nanocomposite for Efficient Removal of Inorganic and Organic Based Water Contaminants – Unravelling the Adsorption Mechanism. *Materials Advances*, **2**(11); 3600–3612

Liu, T., W. Liu, X. Li, H. Wang, Y. Lan, S. Zhang, Y. Wang, and H. Liu (2024). Effect of Environmental Factors on Adsorption of Ciprofloxacin from Wastewater by Microwave Alkali Modified Fly Ash. *Scientific Reports*, **14**(1); 1–13

Memon, N., U. Kanwal, A. Memon, S. S. Memon, and S. Q. Memon (2021). Synthesis, Characterization, and Application of Co-Al-Zn Layered Double Hydroxide/Hydrochar Composite for Simultaneous Removal of Cationic and Anionic Dyes. *Journal of Chemistry*, **2021**; 1138493

Meng, X., X. Liu, D. Zeng, Y. Huang, H. Wang, Z. Li, and C. Yu (2025). Recent Advances in Biomass-Derived Hydrochar for Photocatalytic and Electrocatalytic Applications. *Chemical Engineering Science*, **309**; 121435

Nour, M. M. and H. A. Nabwey (2025). Anchor Biochar from Potato Peels with Magnetite Nanoparticles for Solar Photocatalytic Treatment of Oily Wastewater Effluent. *Catalysts*, **15**(1); 731

Oyebamiji, O. O., A. S. Olaleru, R. B. Oyeleke, and L. N. Ofodile (2025). Evaluation and Characterization of Biochar and Briquettes from Agricultural Wastes for Sustainable Energy Production. *Waste Management Bulletin*, **3**(3); 100198

Palapa, N. R., Z. A. Zahara, R. Mohadi, I. Royani, and A. Lesbani (2024). High Performance of Ni-Al/Magnetite Biochar for Methyl Orange Removal in Aqueous Solution. *Science and Technology Indonesia*, **9**(1); 156–166

Ramadhan, N., A. S. Aliyah, R. J. Sayeri, and N. R. Palapa (2025). A Review on Azo Dyes Removal from Wastewater Using Biochar-Based. *Indonesian Journal of Material Research*, **3**(2); 47–56

Ramadhan, N., M. Mardiyanto, N. Annuria, and Y. Hanifah (2026). Selective Adsorption and Reusability of LDH @ Microalgae (Spirulina) Hydrochar via Microwave-Assisted Synthesis for Ciprofloxacin Removal: Competitive Fluoroquinolone Adsorption and Mechanistic Insight. *Colloids and Surfaces A: Physicochemical and Engineering Aspects*, **739**; 140131

Rath, A., P. K. Sahu, A. Champati, A. Pradhan, A. Madhual, and P. M. Mishra (2025). A Novel Cu–Al LDH / g-C_3N_4 Z-Scheme Photocatalyst for Environmental Remediation of Cresol Red. *Discover Applied Sciences*, **7**; 846

Rohmatullaili, A., N. Savira, D. Erviana, D. Zultriana, R. Mohadi, and A. Lesbani (2024). A Series of MgAl Layer Double Hydroxide-Based Materials Intercalated with Clitoria ternatea Flower Extract as Photocatalysts in the Ciprofloxacin Degradation. *Chemical Physics Impact*, **8**; 100587

Upadhyay, P. and S. Chakma (2024). Physical Insight into the Enhanced Urea Electrooxidation Using Ni and Fe-Based LDH, LDO, and Hydroxides Under Different Dissolved Gas Saturation Conditions in Electrolyte. *International Journal of Hydrogen Energy*, **85**; 744–757

Zahid, M., Z. U. H. Khan, S. Sabahat, M. M. S. Abdullah, N. S. Shah, and N. Muhammad (2025). Photocatalytic Degradation of Norfloxacin Using Biochar Supported nZVMn/TiO_2 Nanocomposite: Synthesis, Characterization, and Performance Evaluation. *Surfaces and Interfaces*, **72**; 107034

Zauška, L., D. Volavka, M. Lisnichuk, T. Zelenka, E. Kinnertová, et al. (2024). Tuning the Photocatalytic Performance of Mesoporous Silica-Titanium Dioxide and Cobalt Titanate for Methylene Blue and Congo Red Adsorption/Photodegradation. *Journal of Photochemistry and Photobiology A: Chemistry*, **451**

Zhang, Z., J. Yang, L. Li, J. Qian, Y. Zhao, and T. Wang (2021). Nitrogen Distribution and Evolution During Persulfate Assisted Hydrothermal Carbonization of Spirulina. *Bioresource Technology*, **342**; 125980

Zheng, D., M. Wu, E. Zheng, Y. Wang, C. Feng, J. Zou, M. Juan, X. Bai, T. Wang, and Y. Shi (2022). Adsorption and Oxidation of Ciprofloxacin by a Novel Layered Double Hydroxides Modified Sludge Biochar. *Journal of Colloid and Interface Science*, **625**; 596–605

